STATUS OF THE TRASCO PROJECT*

Danilo Barni for the TRASCO-AC Group

INFN Milano, LASA, Via Fratelli Cervi 201, I-20090 Segrate (MI), Italy

Abstract

We present the status of TRASCO that is a joint INFN/ENEA program aiming at the design and the technological investigation of the main components of an accelerator driven system (ADS) for nuclear waste transmutation. After a short overview of the main components of the linac we focus on the description of the superconducting high energy sections. An analysis of the design criteria and a discussion of the chosen solution are presented. The actual status of the R&D program and prototyping of the main components are also presented.

1 THE TRASCO INTENSE PROTON SOURCE: TRIPS

The design of the TRASCO intense proton source (TRIPS) has been completed in 1999 and the source has been assembled at LNS in May 2000.

Its task consists in the production of a 35 mA dc proton beam with a normalized emittance below 0.2 π mm mrad at an operating voltage of 80 kV. The source is based on the principle of off-resonance microwave discharge [1].

The microwave matching system is a four step maximally flat transformer, a system to move the coils on-line has been implemented, but mainly the efforts have been concentrated on the extraction system with the aim to increase the source availability and reliability, in order to meet the requirement of a driver for an ADS system.

The choice of an off-resonance microwave discharge ion source has been motivated by the requirements of high yield, high proton fraction and long-term stability.

The results obtained in August (55 mA with a proton fraction of 90%) confirmed that the TRIPS design could be reliably achieved. Low beam emittances has been reached at SILHI by means of controlled gas injection [2].

Therefore the future developments to be done at LNS will concern stability, reliability and reproducibility.

1.1 The TRIPS design

The design of TRIPS is shown in Figure 1. The microwave power obtained with a 2.45 GHz - 2 kW magnetron is coupled to the cylindrical water-cooled OHFC copper plasma chamber (100 mm long and 90 mm in diameter) through a circulator, a four stub automatic tuning unit and a maximally flat matching transformer. The microwave pressure window is placed behind a water-cooled bend in order to avoid any damage due to the back-streaming electrons.

Two magnetic coils, independently on-line moved and energized in order to vary the position of the electron cyclotron resonance (ECR) zones in the chamber, produce

the desired magnetic field configuration. Moreover, the design has been aimed to simplify the operations of maintenance especially in the extraction zone.
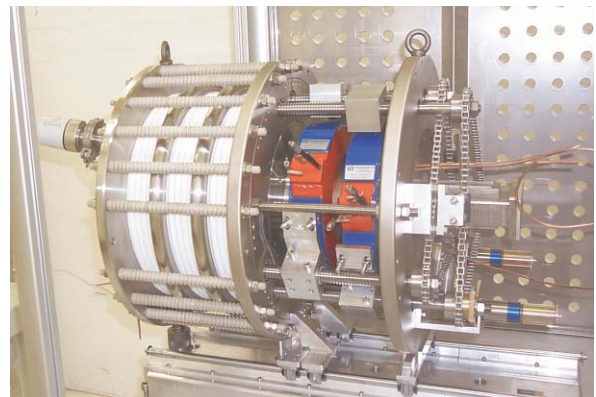

Figure 1: Trips installed on the HV platform in LNS.

In order to optimize the coupling between the microwave generator and the plasma chamber a multisection quarter-wave transformer is used.

The transformer matches progressively the impedances and concentrates the electric field at the center of the plasma chamber, resulting in a significant increase of the extracted current density.

The extraction geometry of the TRIPS source is the result of several studies on the SILHI extraction system. The configuration chosen for SILHI was the pentode, and in the last two years different solutions have been tested on the source according to the calculations done. The last configuration calculated permitted to obtain in the long run test of 104 h (October 99) the outstanding availability of 99.96% (only one spark occurred) [2].

The gaps, the voltage and the extraction holes have been modified in order to reduce the length of the extraction zone where the beam is uncompensated and to reduce the aperture-lens effect. Beam dynamics simulations have been performed and RMS normalized emittance below 0.2 π mm mrad (including the beam halo) have been calculated. The trajectory plot of the extraction system of TRIPS is shown in Figure 2.

1.2 Source status

The 100 kV high voltage platform is operational and the first section of the low energy beam transfer line (LEBT) necessary for the beam analysis and characterization has been assembled. The LEBT line consists of a solenoid to provide the necessary beam focusing, a four sector ring to measure beam misalignments and inhomogeneity.
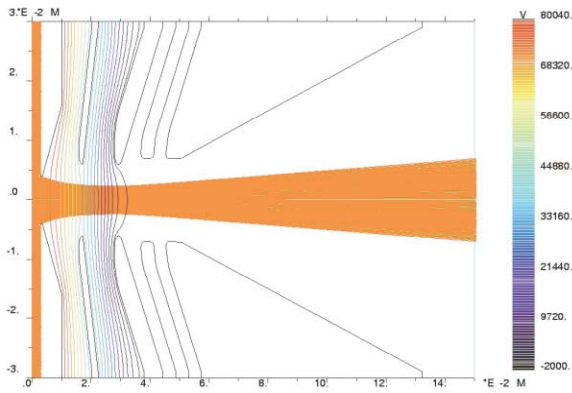
Figure 2.Trajectory plot of the extraction system: extraction voltage is 80 kV and puller voltage is 45 kV

The first plasma has been obtained for the coils parameters (positions and currents) close to the calculated ones and the moving solenoids permit to optimize the ionization process by trying different field profiles.

A first beam of 20 mA at 50 keV has been produced by the source at very low RF power (220 W) in May 2000.

Some failures induced by HV sparks stopped these first promising operations. Different modifications have been made, not only to solve this problem, which is common in this type of sources, but also in order to obtain the long-term reliability requested by the ADS facility.

Last source test produced 60mA at 80kV, and future work will be dedicated to reliability and availability tests and possible improvements [3].

Figure 3. The TRIPS high voltage platform (left) and the first section of the LEBT line.

1.3 Data validation

We have investigated at the SILHI source the more stringent request concerning the reliability in a 12 hours test where the SILHI source was set at working conditions similar to the ones that will be used by TRIPS. The beam availability obtained during this period has been of 99.72 %. During this test only one spark have occured after 80 min. of operations: the extraction and puller power supplies fell down. The beam has been recovered within 2 min. after resetting the computer located on the high voltage platform.

2 THE LOW ENERGY SECTION

The low energy linac, following the microwave discharge ion source, in our nominal design is composed by an RFQ and a superconducting linac (ISCL); at low energy the beam is more sensitive to space charge and in general to perturbations, so that the design and construction of this part of the linac is particularly demanding. Our design choice has been driven by the requirements of reliability (continuity in beam delivery to the subcritical assembly), power conversion efficiency and compactness. The prototypes under construction at LNL are the first third of the RFQ and one of the superconducting cavities, of reentrant-type. As an alternative the option of a normal conducting DTL up to 100 MeV has been considered in detail.

2.1 The TRASCO RFQ

In table. 1 the main RFQ parameters are listed [4]. In particular the beam loading is less then one fourth of LEDA, the 100 mA, 6.7 MeV RFQ commissioned at Los Alamos National Laboratory [5], which is necessarily a point of comparison. The lower beam power makes possible (and necessary) a different optimization of the design. For example, we can use a single klystron and keep a lower power dissipation density in the cavity. The TRASCO 352.2 MHz RFQ has been designed to accelerate relatively high current proton beams (30 mA) with beam losses lower than 4%, to prevent copper activation.

Table 1: RFQ Design Parameter

Parameter	Value
RF Frequency	352.2 MHz
Energy Range	80 keV-5 MeV
Proton Design Current	30 mA
Duty factor	100 %
Maximum Surface Field	33 MV/m
Kilpatrick Factor	1.8
rms Transverse Emittance	0.2 π mm mrad
rms Longitudinal Emittance	0.18 π mm mrad
RFQ Length	7.13 m
Intervane Voltage	68 kV
Transmission @ design current	96%
Modulation	1-1.94
Average Aperture R_0	2.9-3.2 mm
Synchronous Phase	-90 to –29 deg
Q factor (SF/1.2)	8261
Dissipated Power (SF*1.2)	0.579 MW
Beam Loading	0.1476 MW
RF Total Power Consumption	0.726 MW

The main design constraints are determined by the maximum surface electric field, which has been set to 33 MV/m, i.e. 1.8 times the Kilpatrick value at the frequency of 352.2 MHz, and the available RF power, that we set assuming the use of a single CERN/LEP type klystron with a nominal power of 1.3 MW.

2.2 RFQ Design and beam dynamics

The RFQ has been designed with the four traditional sections: the radial matching section, the shaper, the gentle buncher and the accelerator [4].

These design choices have been extensively simulated predicting a beam transmission in excess of 96% for beam currents up to 50 mA, with losses mainly located below 2 MeV. The total power deposited on the structure is approximately 1 kW, with only 210 W at energies above 2 MeV.

Figure 4 shows the longitudinal variation along the RFQ sections of the average aperture R0, the beam aperture a, the focusing parameter B, the modulation factor m, the acceleration factor A, the surface field Es, and the synchronous energy (W_s) and phase (ϕ_s). show the resulting beam dynamics simulations. Simulation shows that a mismatch lower then 6%, a beam misalignment better then 0.25 mm and a source rms. normalized emittance better then 0.23 π mm mrad are required and consistent with the source and LEBT specifications.
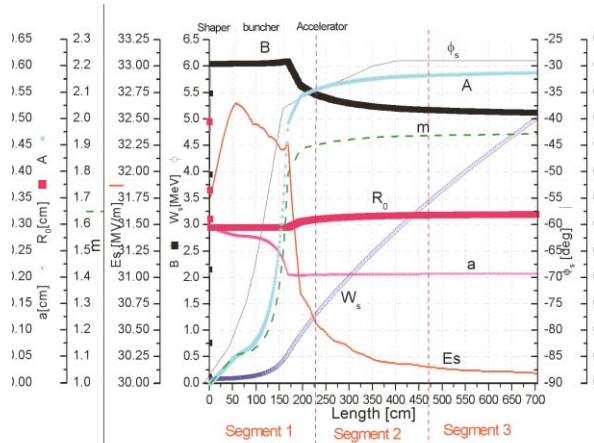

Figure 4. Longitudinal variation of the RFQ design parameters along the three sections.

Each segment will be built in two longitudinal sections and each section is a sandwich of four parts, built in OFE copper, brazed together in a vacuum furnace. Four coupler ports, one in each quadrant and at two longitudinal positions, will feed the RF power.

The RFQ vane tips will be modulated with a high precision milling machine before the brazing; a single tool will be used, with a transverse radius of 2.93 mm. As the average aperture increases in the accelerator section, the RFQ voltage is kept constant and the cut-off frequency is maintained by increasing the transverse section dimensions.

The electromagnetic design has been carried out using 2D Superfish (SF) and 3D (MAFIA) computer simulations. While 2D simulations have been used to determine the basic design and to evaluate power dissipation and frequency shifts due to boundary deformations, the 3D simulations have been used to model the intrinsically 3D details [6].

The thermal behavior of the RFQ cross section has been analyzed using the codes ANSYS and SF. The RF power source used is 1.5 times the SF distribution, for a total of about 1 kW per structure cm.

The mechanical deformation, calculated by ANSYS for the given cooling channels distribution, determines the (local) frequency shift by means of Slater theorem. The heat exchange between water and copper is calculated for the given water velocity (< 4 m/s as a design parameter) and channel shape.

The goal is to keep below 20 kHz (threshold for acceptable field variation) the local frequency shift between RF on and RF off, and between the beginning and the end of a 1.2 m section (water input and output).

In figure 5 we plot the temperature maps and the deformation maps at the beginning (left) and at the end (right) of one RFQ section; both the requirements have been fulfilled.

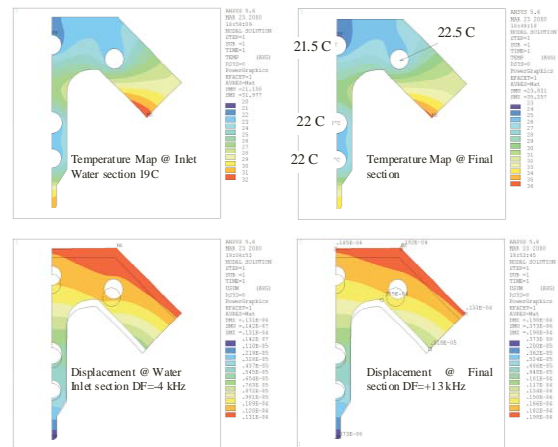The total water flux is of about 3000 liters per minute.

Figure 5. Temperature field (top) and induced deformations (bottom) at two longitudinal positions along one RFQ section (beginning/end of the water channel)

The mechanical construction errors will be much larger than the thermal deformations, so that a correction system to be used a posteriori, (i.e. after the brazing), is needed.

2.3 The reference DTL design

A three section DTL, with transition energies at 20 and 70 MeV has been investigated, at the 352.2 MHz LEP frequency. In each section the quadrupole magnets are identical and geometrical parameters of the RF cavities as the diameter and the beam bore radius are kept constant. The whole linac length is approximately 80 m.[7]

From the constructive point of view the DTL proposed is a standard structure suitable to stand the CW operation. The quadrupoles magnets, housed in the drift tubes, are made in soft iron with high saturation field, with hollow conductors for water-cooling (4 by 3 mm with a 2 mm hole). The drift tubes are realized in bulk copper with an adequate cooling circuit. The dimensions of the tubes are dictated by the quadrupole magnets and by the thickness of the copper wall that has to be large enough to

efficiently transmit the heat generated by the RF dissipation to the cooling circuit. The drift tube dimensions and shape are critical for obtaining a high shunt impedance.

The beam dynamics was simulated with PARMILA code and the DTL aperture is always between 8 and 12 times the beam rms radius, a safe value at these energies.

Due to the low shunt impedance value of the RF structures a 100 MeV, 30 mA linac dissipates approximately 9 MW in the structure, a considerable amount of power that, at these moderate currents, has a non-negligible impact on the whole linac efficiency.

2.4 The superconducting ISCL

A superconducting option for the 5-100 MeV linac is also under study. We considered an Independently phased Superconducting Cavity Linac (ISCL) similar to those used for low energy heavy ions in many nuclear physics laboratories like ours, but at much higher beam intensity, and in a wider beta range. We checked various kind of cavities and we selected the so-called "reentrant cavities", that are modified pillbox, cylindrically symmetric and therefore theoretically dipole free [8].

One of the advantages of this kind of linac is its flexibility, that allows using it CW at lower current or even with different kind of particles, like deuterons. In table 2 we list the main specifications and machine characteristics. In particular we specified the two main constraints of the independently phased resonators: the surface field and the beam loading per cavity. The second constraint is specific of high current machines: in our case we want to feed each cavity with a single solid state amplifier and the limitation to 15 kW is consistent with the present technology.

Table 2.ISCL Design Parameters.

Parameter		Value
Energy range		5-100MeV
Total length		48 m
Synchronous phase		-40
Average acceleration		1.82 deg
Number of cavities		230
Cavity bore radius		1.5 cm
Quadrupole gradient		31 T/m
Quad aperture/length		2/5 cm
Output RMS Emittance	Trans.	0.42 mm mrad
	Long.	0.2 mm mrad
Current limit (losses<10^{-4})		>50 mA
RF dissipation (R_s=100 nΩ, R_{BCS}=58 nΩ)		1204 W (@4.2K)
Beam loading		2.85 MW
RF sys. pwr. cons. (η_{RF}=50%)		5.7 W
Static cryogenic losses (10 W/m)		480 W
Cryo. Consumption (η_{cryo}=1/500)		0.84 MW
Quadrupoles and ancillaries		0.5 MW
Mains power		7.04 MW
Power conversion efficiency		40 %

An additional constraint is given by the reliability requirements typical of an ADS, where the operation with a sub-critical reactor is spoiled even by a beam shut down of a second. To meet these requirements we have chosen an architecture with reliable solid state amplifiers. Even in the presence of a large number of such RF systems with finite reliability, we required that the beam could be transmitted in case of failure of a cavity. This is connected to the requirement that the acceleration per cavity plus the energy spread is smaller than the separatrix energy width. If the beam survives the failure of a single amplifier, and the amplifier can be replaced on line, the resulting availability of the linac is highly improved.

We have chosen a FODO focusing structure with period 8 βλ. As the period becomes longer, a larger number of cavities can be installed between the quadrupoles (figure 6).
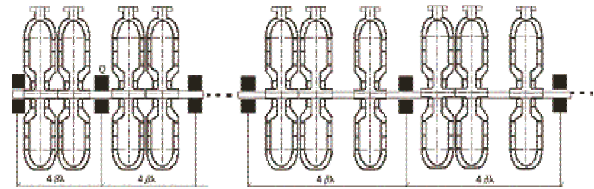

Figure 6. ISCL layout: reentrant cavities and quadrupoles in the cyrostat.

The cavity geometry has been analyzed with the SUPERFISH code, and the main parameters are reported in Table 3 [9]. Since the performances of the reentrant cavities have been limited in the past by the strong multipacting behavior of the pillbox shape with a flattop equator, the cavity shape has been modified with an elliptical equator shape, in order to lower the field levels in the equatorial region.

Table 3 Resonator parameters calculated by means of the code SUPERFISH.

Parameter	Value	Units
Total length	135	mm
Internal length	80	mm
Bore radius	15	mm
Frequency	352.2	MHz
U/E_a^2	0.034	J/(MV/m)2
E_p/E_a	3.05	
H_p/E_a	30.6	G/(MV/m)
$\Gamma = R_s \times Q$	83.9	Ω
R_{sh} (Cu)	18	MΩ/m
β	≥ 0.1	

Since the main limitation in low-β superconducting cavities is usually determined by the maximum achievable surface electric field, related to the onset of field emission, and since our linac design required relatively low energy gain per cavity, we looked mainly for low surface electric and magnetic field, and short physical dimensions.

The RF power will be fed through a inductive coupler, still under study, located on the resonator equator. A deep study of the multipacting (MP) properties of the cavity was performed, with more than 50000 runs of the simulation program TWTRAJ. The region where most of the multipacting levels is concentrated, in the "pillbox" design, is the resonator equator.

Electrons originating in high electric field regions drift to the equator and are collected there, building very strong levels with various multiplicities. This region has been properly shaped with an elliptical contour (ratio between axes 1:1.5) and all high field levels have been finally eliminated. Some results can be seen in figure 7.
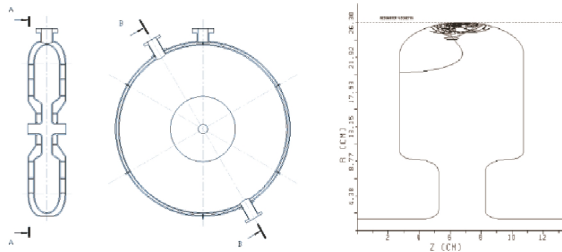

Figure 7. The reentrant cavity mechanical design (left). Example of the multipacting simulation program output (the horizontal axis is stretched in the picture). The circular contour, as well as the rectangular one, was causing high field multipacting levels (right).

The main concern in the mechanical design was related to the large force acting on the relatively flat and wide resonator surface. The niobium sheet, 3 mm thick, could not sustain the pressure in the absence of strong reinforcement.

We tackled this problem using a different approach: in our design, the helium vessel is part of the resonator and is welded to the resonator wall so that the net force on the total structure is nearly cancelled. This design allows a relatively light structure with a good stability and a minimum displacement of the walls under pressure (limited to a few microns) when the tuner is mounted. The mechanical stresses are also confined to rather safe values (figure 8).

The 4.2 K helium is fed by gravity through a flange on the top of the resonator; like in most superconducting linacs for heavy ions, there is no separation between the beam vacuum and the cryostat one.

The tuning is obtained, changing the gap length, by means of a mechanical tuner connected to the external part of the drift tubes. A "nutcracker" type tuner, driven by a piezoelectric or magnetostrictive actuator, is being presently considered. Since the required tuning force is relatively low, the calculated Lorenz force detuning (170 Hz/(MV/m)^2) and helium pressure detuning (140 Hz/mbar) of the bare cavity are not negligible in comparison to the 1 kHz resonator RF bandwidth in operation. A stiff tuner reduces the pressure detuning to ~20 Hz/mbar.

The foreseen CW mode of operation gives a nearly constant radiation pressure on the walls that can be compensated by the tuner. The experimental study of possible mechanical instabilities and of their remedies, however, is one of the aims of this prototype construction. For the design and simulation of the mechanical structure we used the I-DEAS code.
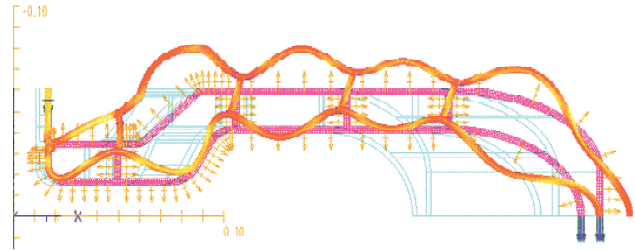

Figure 8. Mechanical deformation as a result of 1 bar pressure increase in the helium bath. The maximum displacement is about 20 μm in the outer shell.

The ISCL design based on reentrant cavities is justified by the constraint of a 0.5 MeV maximum energy gain per cavity; this value is dictated by the requirement of beam transport without losses, with no change of the linac operational parameters, even in case of one cavity failure.

If this requirement can be fulfilled by means of a different method, a cost effective linac design could be based on 2 gap, high gradient superconducting cavities. The number of resonators would be nearly halved; the linac overall length and cost could be reduced significantly.

The beam loading per cavity would reach 30-45 kW, value that would allow the use of the CERN LEP RF couplers technology. This power range is very well covered by commercial klystrode RF amplifiers, that combine a very high efficiency, high gain and good linearity characteristics.

The field distribution in the RF gap of a short QWR contains a dipole component which could cause beam emittance degradation. Studies are being performed in order to minimize this effect, both by geometrical optimization of the cavity shape and by a properly designed linac lattice. The dipole field components are absent in Half-Wave Resonators (HWR), at the price of a more complicated geometry. HWRs performance is expected to be comparable or even superior to QWRs.
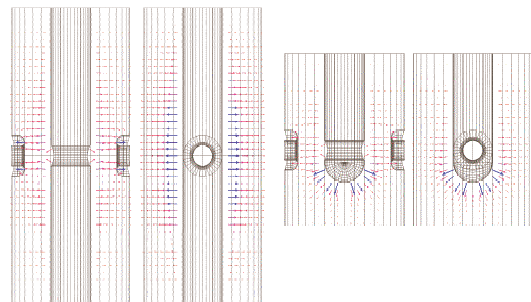

Figure 9. : Models of β=0.25, 352 MHz HWR/QWR.

A specific research activity has been devoted to the investigation of the beam halo formation process The usual approach to the problem is based on multiparticle programs and particle core model (PCM). In the first case one solves the self-consistent problem of the evolution of the whole particle distribution, but the number of particles is limited by computer capabilities. In the second case one simulates the dynamics of test particles in the presence of a given particle distribution; in this way the diffusion of few particles, which does not affect the beam core, can be studied.

We have considered both directions by developing a 3D particle in cell program to solve the Poisson-Vlasov equation and a 3D PCM where the phase space analysis is performed using the frequency map technique [10].

In the next year the FMA and the 3D PIC program will be integrated in a linac design code, able to study both the emittance exchanges and the low probability particle diffusion. Recently, a very fast damping of beam envelope oscillation amplitudes has been observed in simulations of very high intensity beams transportation (initial Gaussian distribution for $\sigma/\sigma0=0.29$) [11].

Several simulations, with the modified multiparticle code PARMT, have been carried out, to point out in which conditions this fast damping occurs and what kind of mechanism could be responsible for it. The explanation found involves the so called Landau damping, i.e. the attenuation of coherent oscillations when the single particle frequencies have a spread.

3 THE SUPERCONDUCTING HIGH ENERGY LINAC

The starting energy of the high-energy superconducting linac has been set in the 90-100 MeV energy range. At energies below this range the decrease in length of the elliptical cavities, and the corresponding decrease in overall performances, favors the choice of either a standard normal conducting accelerating structure or the use of different resonant structure geometries.

3.1 The choice of frequency

The original choice of the 352.2 MHz frequency [12] was motivated by a scenario in which a demonstrator ADS facility was decided to be built as soon as possible (as initially proposed by Carlo Rubbia for the Energy Amplifier/ADS demonstator). At this frequency, in fact, all the required technologies have been proven by the CERN LEP experience, and most of the necessary ancillaries exist with specifications close to the ADS requirements [13]

During the last two years it became clear that the envisaged time scale needed for an ADS demonstration plant will be longer than initially expected, and the bulk niobium superconducting RF technology set by the TESLA/TTF International Collaboration [14] allows the design of better performing cavities with respect to the CERN sputtered technology, that dates back more than a decade.

Doubling the RF frequency to 704.4 MHz, and using the know-how gained by the TTF Collaboration for the development of the missing ancillary components at these frequencies, the superconducting linac length can be nearly halved, using the possibility of operating reliably at almost double accelerating gradients with bulk Nb cavities. The additional complication of operating at 2 K is overcome by this drastic reduction in linac length.

One of the advantages of the 704.4 MHz frequency is that the cavities are 8 times smaller in volume with respect to the CERN cavities, and several infrastructures for cavity fabrication, treatment and measure exist (notably CEA/Saclay) or are being set up (as in INFN Milano/LASA) in Europe. These smaller cavities also show a better mechanical stability (again related to the smaller physical dimensions).

We may conclude that the 704.4 MHz choice leaves more space for making use of the technological improvements obtained in the past years by the TESLA/TFF International Collaboration, as it has been successfully proven by both the single cell $\beta=0.65$ cavities developed by CEA/Saclay and the single-cell $\beta=0.5$ cavity that we have built for TRASCO.

3.2 Technological activities for the cavity production

Two parallel experimental activities have been followed in order to assess the feasibility of both frequency options. The first activity, in collaboration with CERN, aimed at reaching the same LEP cavity performances with a $\beta=0.85$ sputtered cavity, the other aimed at proving the reliability of the bulk Nb technology for the low $\beta=0.5$ cavities.

For the Cu-Nb sputtered program, one single cell and one five cell $\beta=0.85$ cavity have been built and tested by CERN with the TRASCO design at 352.2 MHz, with results exceeding the design specifications. The results for two series of tests of the five-cell cavity, before and after He processing, are shown in figure 10. The upper horizontal axis shows the peak magnetic field on the surface (directly proportional to the Eacc). The ratio of the peak surface fields with respect to the accelerating field depends entirely on the cavity geometry and is higher for lower β cavities than for electron ($\beta=1$) cavities, like the LEP II cavities. Taking into account this fact the Q vs. Bpeak curve of the TRASCO $\beta=0.85$ cavity measurement falls entirely in the production spread of the last LEP II cavities batch. The dashed area in the figure indicated the operating region of the cavities, with a design value of $Q=2\times10^9$ at the accelerating field of 6.5 MV/m.

An ongoing extension of the agreement with CERN allowed us to equip the cavity with a He tank, the standard LEP tuner, coupler and HOM, install it in a specially modified spare cryomodule, and test it in the LEP cryomodule test bench.
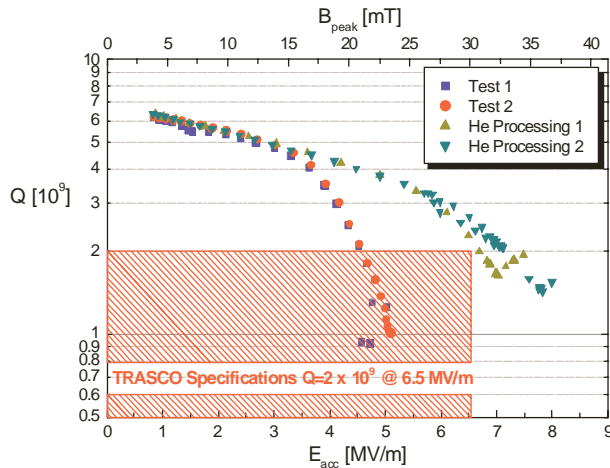
Figure 10. Picture and Q vs. Eacc plot of the β=0.85 Nb/Cu five cell cavity tested at CERN.

For the Bulk Niobium program, two single cells β=0.5 cavity has been manufactured by one of the TRASCO industrial partners (Zanon) using the low-grade (reactor grade, with minimal RRR=30) niobium sheets that we purchased mainly for the test of the deep drawing dies. After e-beam welding the cavities have been sent to CEA/Saclay for the chemical treatments and RF tests. Due to the low quality of the Nb sheets, the cavity were not expected to reach high fields. However, the tests at Saclay were very successful and reliable, and both cavities performed very well above the design specifications of a $Q=1\times10^{10}$ at the accelerating field of 8.5 MV/m, as shown from figure 11. Moreover, the Q factor does not exhibit any significant slope up to fields greater than the nominal operating field [15].

The residual resistivity ratio estimated from the RF measurements is RRR=58. After reaching an accelerating field value of 10.5 MV/m the cavity abruptly quenched. The cavity will be tested again in Milan when the cavity test area is operational. Zanon has also manufactured two additional single cell cavities high quality (RRR=250) niobium sheets. These cavities will be prepared and test in Saclay and at Jefferson Lab.

After these single-cell cavity prototypes one or two five-cell cavities will be built and tested.

3.3 RF Test Bench in Milan

As part of the TRASCO_AC program, a cavity RF test bench has been set up and is under commissioning in Milano/LASA [16]. The system is composed by a vertical cryostat that allows testing cavities with frequencies in the range from 500 to 800 MHz (a special insert for the short beta 704.4 MHz cavities has been installed in an existing cryostat that has been used for the 500 MHz cavities of the INFN ARES program) and an RF power generator that delivers 500 W in the same band. This system however, does not allow breaking the cavity vacuum without contamination, and is ready to receive cavities for testing only if the RF antennas have already been mounted in clean conditions before sealing the

cavity. As planned for the extension of the TRASCO program, a class 100 clean room for the high pressure rinsing with ultrapure water and for the cavity preparation before the tests (mainly assembling of the RF antennas for the measurements) has been designed and will be delivered in autumn 2001, rendering the test facility fully operational. A contact with a local company for the Buffered Chemical Polishing (BCP) of the Nb cavities has been established, with the aim of acquiring complete control of the cavity preparation steps from its fabrication in Zanon to the tests in Milan.
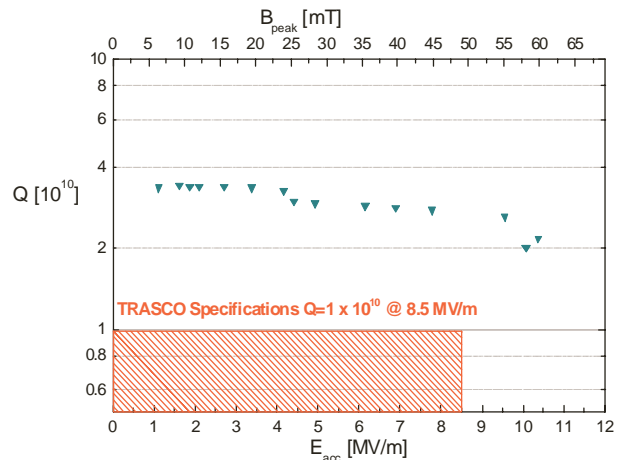

Figure 11. Q vs. Eacc curve of the β=0.5 bulk Nb single cell cavity.

3.4 Alternative schemes for cavity stiffening

While the superconducting cavity design for TRASCO is fully consistent with CW operation, in the case of the proposed pulsed operation, in view, for example, of a multipurpose machine the Lorentz force detuning coefficient of the lowest beta cavity is probably too high. As for TESLA, an improvement of this crucial parameter is strictly related to the machine cost because of the impact on the RF power distribution and the low level RF controls.

In the framework of the MOU between INFN, CEA and IN2P3, in collaboration with the CESI laboratories in Milano and Saes Getters, we have studied and analyzed the thermal and mechanical characteristics of bimetallic niobium-copper samples produced with different deposition techniques [17] and thermal treatments. The sample thermal conductivity (parallel and normal to the deposition direction) has been tested at room and at cryogenic temperatures, for a modified arc technique, called "Pure-Coat". The results are very promising, indicating a suitable conductivity, at least for the moderate-field required by the proton cavity parameters.

The mechanical properties (Interface cohesion, Young modulus, yield stress and elongation) have been measured using different techniques (pull out, four point bending, Brinnel hardness test, thermal shock). The Young modulus and yield stress of the last samples are compatible with the required stiffening material

specifications. The initial problem of an extreme brittleness of the deposited copper, showing an elongation before rupture of less than 0.2%, is being solved through a well-calibrated heat treatment under vacuum. A value of 2% has already been measured on the treated samples.

The technological analyses are crosschecked with physical tests (SEM, Auger and XPS), to obtain a correlation between the material structure, its composition and the physical behavior. The results of the analysis are fed back for the optimization of the deposition procedures and of the surface treatments.

3.5 Conceptual design of the TRASCO Cryomodules

The design of the cryomodule [18] needs to be based mainly on the ADS requirements in terms of reliability and system engineering.

The cryomodule reliability is dominated by the vacuum (insulation, coupler and beam) system and by the helium cooling distribution. Fast access to the module and easy repairing, during maintenance time, complete the requirements. To achieve these requirements the cryomodules we are designing are completely independent from each other. The cryogenic transfer line runs along the modules string and the connection boxes link the modules to the He supply. Vacuum ports and RF distribution have also their own connections. Each cryomodule can be physically separated from the line with no perturbation on the working condition of the others.

To ensure good RF cavity performances the cavities need to be completely assembled in good cleaning condition (at least class 100 clean room) and all the connections to external ports have to be closed in the clean room.

The power coupler is another critical component that needs to be completely assembled and closed in the clean room. These constraints result in the necessity of considerable clearance space to fix the cold mass (that is the cavity string with the couplers and the thermal shields) in the vacuum vessel. The operation has also to prevent the alignments.

On the basis of the criteria expressed before, we have produced a conceptual design of the TRASCO cryomodule [18]. The design includes solutions that have been used and tested for the TESLA/TTF cryomodules, like the cavity sliding supports, that allow a semirigid coupler solution, or the G10 fiberglass supports sustaining the cold cavity string and the thermal shields to a stiff room temperature frame. The vacuum vessel of the cryomodule has a large lateral flange that allows a lateral sliding of the fully assembled cold mass on the support frame, by means of rails (see figure 12).

The necessary assembling and alignment procedures have been identified and outlined, and follow the experience gained in the fabrication, assembly and installation of the TTF cryomodules in DESY.
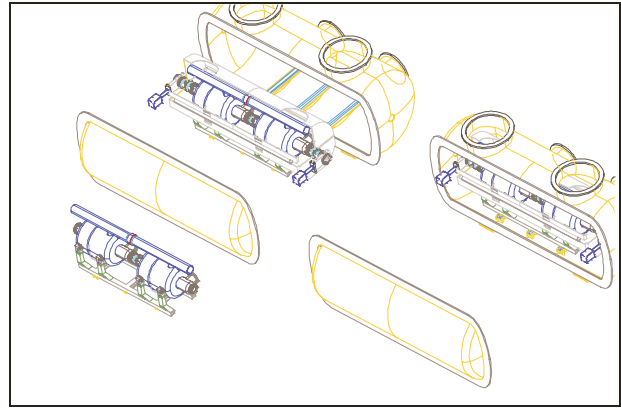

Figure 12. The cavities string (on the left) is assembled and closed in a class 100 clean room. The system is aligned and the cold mass is assembled. The rail-sled system allows to preserve the alignment during the cold mass insertion into the vacuum vessel.

3.6 Conceptual design of the linac and beam dynamics studies

The TRASCO_AC activities for the superconducting high energy linac include the choice of a reference configuration for the linac beamline components and the beam dynamics studies aimed at the validation of the proposed configuration. The theoretical design activities have been focused mainly on two subjects:

- The "optimal" design of the superconducting cavities [19]
- The beam optics and beam dynamics studies [20].

In order to determine a cavity geometry that has the necessary electromagnetic and mechanical performances required by the linac design, we have used a geometry parametrization that allows easily to balance the peak electric and magnetic fields and to control the cavity mechanical properties. The cavity geometry is elliptical both at the equator and at the iris, and has been parametrized in a way that each geometrical parameter allows the control of a single cell electromagnetic (or mechanical) parameter.

A set of computer codes has been written in order to allow the automatic execution of standard RF cavity analysis codes (as SUPERFISH) and structural analysis codes (i.e. ANSYS) on the chosen geometry.

With the aid of these analyses and tools, and in close collaboration with the CEA/Saclay and IN2P3/Orsay groups working at the design of the ASH proposal, we defined the cavity shapes for the TRASCO (and ASH) cavities [21]. These are the shapes used for the cavity prototyping activities in Milano and in Saclay. The main cavity geometrical and electromagnetic parameters are reported in table. 4.

A few guidelines imposed by either technological limitations or first order beam optics considerations have been followed in the definition of the linac reference design, and it is worth summarizing them in the following paragraphs.

Table. 4: Main cavity parameters.

Geometrical Parameters			
Synchronous beta	0.50	0.68	0.86
Number of cells	5	5	6
Cell. Length [mm]	100	140	180
Geometrical beta	0.470	0.658	0.846
Full Length [mm]	900	1100	1480
Iris diameter [mm]	80	90	100
Coupler Tube $\varnothing$ [mm]	130		
Internal wall angle,[°]	5.5	8.5	8.5
Equator ellipse ratio, R	1.6	1	1
Iris ellipse ratio, r	1.3	1.3	1.4
Full cavity electromagnetic Parameters			
Max. Epeak/Eacc	3.59	2.61	2.36
Max. Bpeak/Eacc	5.87	4.88	4.08
Cell coupling [%]	1.34	1.10	1.28
R/Q [Ohm]	159	315	598

The energy range from about 90-100 MeV up to 1-2 GeV can be efficiently covered with three sections, i.e. with three different cavity types. A larger number of sections would imply a wider cavity R&D activity for a smaller number of production cavities, while a smaller one would lead to inefficient use of the cavity transit time factor.

The transition energies between the sections have been (loosely) set to 200 MeV and 500 MeV, independently on the optimization of the input energy (say from 85 to 100 MeV) and from the output energy (from 1 to 2 GeV).

The number of cavities per section has been derived using a conservative value of 50 mT for the peak surface magnetic field. The number of cells has been chosen to be 5 in the two lowest beta sections and 6 in the highest beta section.

The transverse focusing lattice is formed by an array of quadrupole doublets, with the cavity cryostats in the long drift between quads. The cryostats contain 2 cavities in the two lowest beta sections and 4 cavities in the highest beta. With these choices the doublet periodicity in the three sections is 4.2, 4.6 and 8.5 m, respectively, and the quadrupole doublets are located in a 1.6 m warm section between the cryomodules. Table. 5 lists the main parameters of the linac sections for the 1 GeV and the 2 GeV linac cases.

The beam line design and matching has been investigated and analyzed with a number of different beam optics codes, either standard design codes available in the accelerator community or tools that have been developed for the proton linac studies in Milano or Saclay [15]. These codes allowed to set the desired transverse phase advances law, and the matching conditions at the linac entrance, and between the linac sections, that are needed to minimize the emittance growth that can lead to undesired beam losses.

We have specially written a beam dynamics code46) for the simulations of the SC TRASCO linac (SCDyn), which advances particles in phase steps through the beam line elements of the linac.

Table 5 : Main SC linac section parameters.

	#1	#2	#3
			1-2 GeV
Section β_S	0.50	0.68	0.86
Section Length [m]	84	124.2	110.5-297.5
Input Energy [MeV]	85	200	500
Focussing Period [m]	4.2	4.6	8.5
# Focussing Periods	20	27	13-35
Max Gain/Cav [MeV]	3.3	6.0	11.4
Max Eacc [MV/m]	8.5	10.2	12.3
# Cells/Cavity	5	5	6
# Cav/Section	40	54	52-140
# Cav/Cryomodule	2	2	4
# Module/Klystron	1	1	1
Max RFCoupler [kW]	66	120	228

The space charge calculations in SCDyn are performed with a cloud in cell charge deposition scheme and a 3D V-cycle multigrid Poisson solver in the beam rest frame. We have extensively used SCDyn for the validation of the TRASCO linac design, and made comparisons with other beam dynamics codes, notably Parmila (Los Alamos) and Partran (Saclay). In figure. 13 we show the behavior of the rms beam sizes along the beam line, for a 1 GeV linac case, corresponding to the same matched case of the previous figure. The beam sizes shown in the figure are the rms envelopes evaluated from the SCDyn multiparticle simulations.
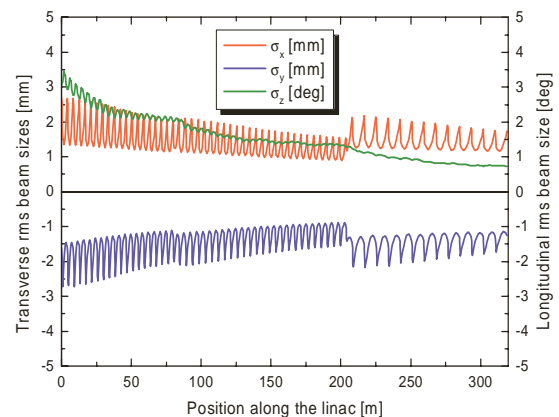

Figure. 13: rms matched beamsizes in the 1 GeV linac, from the SCDyn simulations.

Finally, figure 14 shows the phase spaces of the output beam from the SCDyn simulations, at 1 GeV, for a 50,000 particles simulation. The two ellipses drawn on the phase spaces indicate the rms emittance and 4 times the rms. The characteristics rectangular shape of a space charge dominated beam can be clearly seen in the horizontal phase space (top left). Mismatched case up to a mismatch factor of 30% have shown the onset of filamentation effects that increase the beam emittances, but no evidence of unbounded orbits (that result in beam halos) could be seen from the simulations.
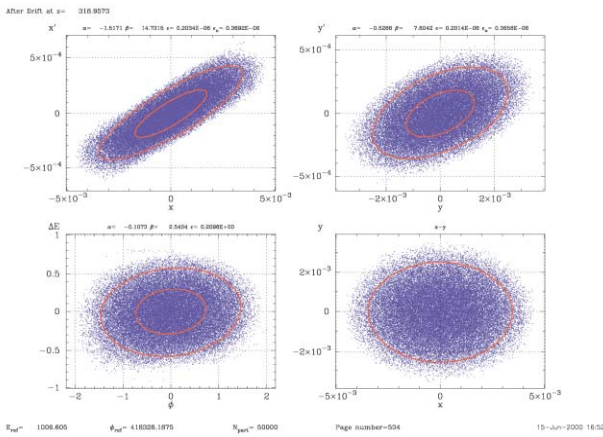
Figure 14. The phase spaces of the output beam (for a 50 k particle simulation).

4 CONCLUSIONS

We have described here the status of the activities of the TRASCO_AC program. We have outlined a reference solution for all the components of the accelerator and we have achieved significant experimental results. A prototype of the TRIPS source has delivered its first beam in LNS, with specifications of the design values. An aluminum model of the RFQ has been built and tested, while the technological model of the RFQ and a prototype reentrant cavity are in fabrication. Both a five-cell high beta, 352.2 MHz, Nb/Cu cavity, built and tested at CERN, and a low beta, 704.4 MHz, bulk Nb single-cell cavities, built by Zanon and tested at Saclay, have met the design specifications in experimental tests.

5 REFERENCES

[1] L. Celona et al. "TRIPS: The high intensity proton source for the TRASCO project", Review of Scientific Instruments, Vol 71 n.2, (2000), p. 771.

[2] L. Celona et al. "Third Activity Report on SILHI Ion Source (June 07 - July 02, 1999)", DAPNIA/SEA/IPHI 99-52.

[3] G. Ciavola et al. "First Results from the Trasco Intense Proton Source (TRIPS) at INFN-LNS", to be published in ICIS01 Proceedings.

[4] M. Comuniam et al. "TRASCO RFQ design", EPAC'2000, Vienna, Austria, p. 927.

[5] D. Schrage et al. "A 6.7 MeV CW RFQ Linac", PAC'97, Vancouver, CA, p. 1093.

[6] M. Comuniam et al. "TRASCO RFQ", Linac 2000, United States, Contribution THD02.

[7] A. Pisent et al., "The DTL approach for a 100 MeV CW linac", 1996, INFN/LNL Report.

[8] A. Pisent et al., "TRASCO 100 MeV high intensity proton linac", EPAC 2000, Vienna, Austria, p. 857.

[9] A. Facco et al., "A Superconductive, Low Beta Single Gap Cavity for a High Intensity Proton Linac", Linac 2000, United States, Contribution THD11.

[10] G.Turchetti et al., "3D solution of the Poisson-Vlasov equations for a line of FODO cells", ICAP2000, Darmstadt, Germany

[11] V. Variale et al., "Fast Damping in Beam Envelope Oscillation Amplitudes of mismatched high intensity beams", EPAC 2000, Vienna, 2000.

[12] C. Pagani et al., "A High Current Proton Linac with 352 MHz SC Cavities", LINAC96, Geneva, Switzerland.

[13] E.Chiaveri, "Production by Industry of a Large Number of Superconducting Cavities: Status and Future", RFSC Workshop 1995, Gif Sur Yvette, France,1995.

[14] C. Pagani et al., "Status and Perspectives of the SC Cavities for TESLA", Advances in Cryogenic Engineering, V 45A, 2000, p. 881.

[15] "5th Meeting on High Power Superconducting Proton Accelerator for Nuclear Waste Transmutation", IPN Orsay, 2000.

[16] C. Pagani, "Superconducting RF activities at INFN Milano-LASA", RFSC Workshop 99, Los Alamos, United States.

[17] S. Bousson et al.,"A New Fabrication and Stiffening Method of SRF Cavities", EPAC 1998, Stockholm, Sweden.

[18] D. Barni et al., "Conceptual design of the cryomodule for the TRASCO SC linac", EPAC 2000, Vienna, Austria.

[19] D. Barni et al., "SC Cavity design for the 700 MHz TRASCO linac", EPAC 2000, Vienna, Austria.

[20] P. Pierini et al., "Validation of the 700 MHz TRASCO SC linac design by multiparticle simulations", EPAC 2000, Vienna, Austria.

[21] J.L. Biarrotte et al., "704 MHz superconducting cavities for a high intensity proton accelerator", RF SC Workshop 99, Los Alamos, United States.